Influence of metakaolin characteristics on the mechanical properties of geopolymers

C. Kuenzel[a,b], T.P. Neville[c], S. Donatello[d], L. Vandeperre[b],

A. R. Boccaccini[b,e], C. R. Cheeseman[a*]

[a]Department of Civil and Environmental Engineering, Imperial College London,

South Kensington Campus, London SW7 2AZ, United Kingdom

[b]Centre for Advanced Structural Ceramics, Department of Materials,

Imperial College London, South Kensington Campus, London SW7 2AZ, United Kingdom

[c] Centre for CO_2 Technology, Department of Chemical Engineering,

University College London, Gower Street, London, WC1E 6JE

[d]Cement and Materials Recycling Department,

Eduardo Torroja Institute of Construction Sciences, Madrid, 28033, Spain

[e]Institute of Biomaterials, University of Erlangen-Nuremberg,

Cauerstrasse 6, 91058 Erlangen, Germany

* Corresponding author: c.cheeseman@imperial.ac.uk

Tel: ++44 (0)207594 5971, Fax: ++44 (0)207 594 6124

Abstract

The relationship between the properties of geopolymers and the characteristics of metakaolin samples used in their preparation has been investigated. Three commercial metakaolin samples have been characterised using ^{27}Al-NMR to determine the coordination number of Al (IV, V and VI), and by acid and alkali dissolution to determine the reactive Si and Al content. The setting and mechanical properties of geopolymers formed from the metakaolin samples under identical conditions are reported, using Weibull statistics to analyse strength data. Although the metakaolin samples contained different levels of five coordinated aluminium (Al (V)) the mechanical properties of the geopolymers formed were very similar. The reactive fraction of metakaolinite determined by dissolution in 8M NaOH provides the most relevant long-term indicator of geopolymer performance.

Keywords: Metakaolin; Geopolymer; Reactive content; Weibull Statistics

1. Introduction

Geopolymers made from a range of different aluminosilicates that have received significant attention in recent years (Komnitsas and Zaharaki, 2007, Khale and Chaudhary, 2007, Duxson et al., 2007a). Forming geopolymers involves mixing an aluminosilicate with highly alkaline activating solution to form a flowable paste. Dissolution/precipitation reactions cause the paste to harden to a solid geopolymer network structure that can have excellent mechanical properties. The majority of geopolymer research has investigated the use of coal fly ash, blast furnace slag and metakaolin (MK) based systems (Somna et al., 2011, Kuenzel et al., 2012). Coal fly ash and slags are relatively cheap and readily available industrial by-products, but they exhibit significant variations in chemical and physical

properties. MK is produced by controlled calcination of naturally occurring kaolinite, and has the advantage of consistent chemical composition and properties. Coal fly ash and slag-based geopolymer concretes are proposed as alternatives to Portland cement concrete and have potential to reduce the carbon footprint of construction (Palomo et al., 1999b, van Jaarsveld et al., 2004, Hardjito et al., 2004, Chindaprasirt et al., 2007,). More expensive MK based geopolymers have been investigated for use in specialist applications such as the encapsulation/immobilisation of nuclear wastes, where chemical/physical property consistency and long-term availability of raw materials is required (Perera et al., 2005, Perera et al., 2006, Blackford et al., 2007, Bell et al., 2009a, Bell et al., 2009b, Kuenzel et al., 2010). Additional important geopolymer properties are excellent resistance to fire and bacterial attack, and the development of rapid early strength (Hermann et al., 1999, Palomo et al., 1999b, Cheng and Chiu, 2003).

Although the chemical composition of MK is generally consistent, very little has been reported on the comparative performance of geopolymers made from different MK samples or the desirable characteristics of MK for geopolymer production. International standards are not currently available to regulate production of MK from kaolinite and therefore the content of reactive Al and Si can vary significantly due to changes in feedstock purity and processing conditions (Sanz et al., 1988).

An important factor that determines the reactivity of MK is reported to be the Al coordination number (Davidovits, 2008). This can be tetrahedral (IV), pentahedral (V) or octahedral (VI). Despite relatively little supporting data it is generally accepted that the quantity of Al (V) in MK influences the mechanical properties of geopolymers (Sagoe-Crentsil and Weng, 2007) and increases MK reactivity. However, the authors are not aware of previous research that has directly correlated Al (V) content with the content of reactive Al

as measured by HF or NaOH dissolution, and the resulting geopolymer properties (Ruiz-Santaquiteriaet al., 2011).

Compressive strength is a basic characterisation property for geopolymers, although comparing results can be difficult due to variations in specimen size, test geometry, loading rate, testing apparatus and mixing/curing procedures used (Proviset al., 2005). Analysis of strength data using Weibull statistics allows prediction of failure probability under a given applied load and requires test data from between 20 and 30 samples to give accurate results (Khalili and Kromp, 1991). Using Weibull statistics in combination with fracture toughness data also allows the critical defect size to be determined.

The aim of the research was to investigate how the characteristics of MK samples influence the setting reactions and mechanical properties of geopolymer paste samples.

2. Materials and Methods

2.1. Materials

Three different MK samples have been characterised and used to form geopolymers under identical processing conditions. The MK samples used were MetaStar 501 (Imerys, UK), Argical M1200 (Imerys, UK) and MetaMax, (BASF, Germany). These were characterised using X-ray fluorescence (XRF, Spectro 2000 XRF analyser, Germany) and loss on ignition. Particle size distribution data was determined by laser diffraction (Beckman Coulter LS100, USA). The crystalline phases present in the MK samples were determined by X-ray diffraction (XRD, PAN analytical X-Pert Pro MPD, Philips, The Netherlands). Samples were analysed using a stepwise scan from 15 to 60 2θ with steps of 0.033º and 20 seconds per step. The CuKα radiation was generated at 40 kV and 20 mA.

2.2. Al coordination and dissolution analysis of MK samples

The coordination number of Al in the MK samples was determined using solid ^{27}Al-MAS NMR (Advance 600 solid state NMR, Bruker, Germany) at room temperature with a resonance frequency of 104.3 MHz and spinning rate of 12 kHz. In order to determine the relative amounts of IV, V and VI coordinated Al, spectra were analysed using the computer program dmfit and by applying a Gaussian model to the peaks (Massiot et al., 2002).

A range of different dissolution techniques have been proposed to determine the reactive Al and Si content in MK (Fernández-Jimenez et al., 2006, Ruiz-Santaquiteria et al., 2011). In this study the amount of reactive Al was determined by dissolving MK samples in either 1% HF or 8 M NaOH and analysing the resulting insoluble residue (Ruiz-Santaquiteria et al., 2011). 1 g of each MK was mixed with 100 ml of 8 M NaOH or 100 ml 1% (mass) HF solution for 20 hours at ambient temperature prior to separating the residual solids by filtration. Previous work has shown that 20 hours is sufficient to dissolve all the reactive phases in MK under these conditions (Kuenzel, 2013). The residual solids collected on ash free filter paper were washed in deionised water until the pH of the filtrate was neutral. The mass of retained solids was determined by calcining the filter paper and retained solids at 1000 °C for 1 hour. Separate fractions of the filtered solids were also dried at 110 °C and analysed by XRD to determine the changes in the crystallinity of MK caused by the dissolution process.

2.3. Preparation of MK geopolymers

All MK geopolymers were prepared using a molar Al:Si:Na ratio of 1:2:1. This is reported to be an ideal Al:Si ratio to produce geopolymers with good mechanical properties (Duxson et al., 2005; 2007b; 2007c). The molar H_2O:Al ratio used was 8 in order to obtain a low viscosity mix. Previous studies have varied the molar H_2O:Al ratio between 5.5 and 12

(Rowles and O'Conner, 2003, Duxson et al., 2005; Fletcher et al., 2005, De Silva et al., 2007, Duxson et al., 2007b, Poulesquen et al., 2011).

Alkali activating solutions were prepared using sodium silicate (26% SiO_2/8% Na_2O, VWR International, Pennsylvania, USA) and sodium hydroxide pellets (NaOH, Fischer Scientific International, New Hampshire, USA) dissolved in deionised water to give the required Si and Na ratio. Activating solutions were prepared by mixing appropriate quantities of Na_2SiO_3 solution with water and NaOH and stirring for 24 hours. The activating solution was then mixed with MK using an automatic mixer (65-L0006/AM, Controls, Italy) for 3 minutes and the slurry cast into stainless steel moulds (10 x 10 x 50 mm). A vibrating table was used for 10 minutes to remove air bubbles, with the samples then placed in sealed polyethylene (PE) bags and cured at ambient temperature (22 ± 3 °C). After two days the samples were de-moulded and placed in sealed PE bags and cured for a further 54 days at ambient temperature.

2.4. Characterisation of geopolymer samples

Setting under ambient conditions was monitored using a Vicat needle penetrometer (Vicatronic Automatic Single Station Vicat Needle Apparatus, Qualitest, USA) following BS EN 196-3 (Standard, 2008). Due to the water soluble nature of MK pastes at very early ages, oil was used instead of water to cover the sample and prevent surface drying during setting.

Isothermal conduction calorimetry (Wexham Developments Ltd., UK) was used to determine the heat output during the dissolution and poly-condensation reactions that characterise the geopolymerisation process, with the external temperature maintained at 20.0 ± 0.1 °C.

Compressive strengths of geopolymers were measured on 10 mm cube samples cut from the original samples (Zwick/Roell Z010, Germany). The crosshead speed was 0.5 mm/minute and the edges of the specimen were lightly chamfered prior to testing.

Flexural strength and fracture toughness were determined using three point bend testing of 10 x 10 x 50 mm samples using a crosshead speed of 0.5 mm/minute and a support span of 40 mm. Before measuring the flexural strength, the edges of samples were lightly chamfered.

The 10 x 10 x 50 mm geopolymer samples were notched using a 0.2 mm thick diamond blade to a depth of approximately 2 mm to measure the fracture toughness (K_{1c}). The K_{1c} was calculated using the following equation (Rooke and Cartwright, 1976):

$$K_{1c} = \frac{3PL\Psi\sqrt{\pi a_0}}{2bW^2} \quad (1)$$

where P = force, L = span length, a_o= notch depth, b = sample width, W = sample height, and Ψ is given by the following equation:

$$\Psi = 1.11 - 1.55\left(\frac{a_0}{W}\right) + 7.71\left(\frac{a_0}{W}\right)^2 - 13.5\left(\frac{a_0}{W}\right)^3 + 14.2\left(\frac{a_0}{W}\right)^4 \quad (2)$$

The statistical behaviour of strength was modelled using the Weibull function (Weibull, 1951). The probability of failure P_f can be described by the following equation:

$$P_f = 1 - exp\left[-\left(\frac{\sigma}{\sigma_0}\right)^m\right] \quad (3)$$

where *m*, the Weibull modulus, is related to the scatter of strength values during a test (Lawn and Wilshaw, 1975) with higher *m* indicating reduced scatter, σ_o is the reference strength and

σ is the nominally applied stress. This equation contains two unknowns, *m* and P_f. To determine P_f, Lawn suggested using the mean rank. However, for tests limited to less than 50 samples the following equation was proposed (Bergman, 1984, Masson and Bourgain, 1992):

$$P_f = \frac{i-0.5}{N} \quad (4)$$

where *N* represents the total number of samples and *i*, each individual sample. The Weibull parameter can then be calculated by combining and rearranging Equations 3 and 4 to give:

$$ln\left[ln\frac{1}{(1-P_f)}\right] = m\ln\left(\frac{\sigma}{\sigma_0}\right) \quad (5)$$

3. Results

3.1. Characterisation of MK samples

The chemical composition of MK (Table 1) shows that all the samples have similar bulk composition. The particle size distributions of the MK samples are shown in Figure 1 and these are also similar. This is important because the MK particle size is reported to influence the mechanical properties of geopolymers (Rahier et al., 2007a). XRD data for the as-received MK samples is shown in Figure 2. All show the expected characteristic background hump between 20º and 30º 2θ associated with an amorphous phase with peaks also associated with crystalline SiO_2 and residual kaolinite.

The extent of dissolution of the MK samples in 1% HF and 8 M NaOH is given in Table 2. The 1% HF caused consistently more dissolution than 8M NaOH. All three MK samples

contained high proportions of reactive material, although Argical MK had significantly lower content of reactive Al and Si due to the quartz present in this sample (Figure 2). XRD data for Argical MK before and after HF attack is presented in Figure 3. HF removes the amorphous phase in MK associated with the intensity background between 20 and 30 degrees 2θ, with the remaining sample consisting of crystalline phases present as impurities.

Composition data obtained by XRF of the Agrical MK sample before and after dissolution in 1% HF or 8M NaOH (Table 3) supports the XRD data, with quartz detected as the dominant component in the insoluble residue. The amount of SiO_2 was lower in Agrical MK after dissolution in 1% HF compared to 8M NaOH and this implies that HF treatment may result in small but significant quartz dissolution via conversion to SiF_4 or intermediate species. The TiO_2 in the insoluble Agrical MK residue highlights the inert nature of this oxide. The NaOH Argical MK residue had significant Al_2O_3 (~20 mass %), a major part of which can be attributed to kaolinite impurities (Figure 3), which appear to be reasonably resistant to HF attack.

When Al:Si:Na:H_2O ratios are selected it is normally assumed that 100% of the Si and Al content in MK is reactive and contributes to geopolymer formation. The data has shown that this assumption is incorrect for Argical MK. Taking into account the insoluble residue mass and the quantities of reactive material released by NaOH dissolution, the actual Al:Si:Na:H_2O ratio was calculated to be 1:1.9:1.1:8.9. Therefore a new Argical based MK geopolymer sample with the correct molar ratio (1:2:1:8) was prepared by adding additional silicate and this is subsequently labelled Argical* MK.

^{27}Al NMR was used to determine the Al in different coordination states. Results (Figure 4) were used to calculate the percentages of Al in different coordination (Table 4). The Al (V) content was found to vary from ~44 to 86% in different MK samples giving a potential reactive content in the order:

MetaMax MK > Argical MK >> MetaStar MK

However, the dissolution results (Table 3) show the following order:

MetaMax MK = MetaStar MK >> Argical MK

3.2. Influence of MK on setting and isothermal calorimetry data

The Vicat needle penetrometer data of the geopolymers (Figure 5) indicates that relatively high mix water ratio (H_2O:Al = 8) minimises differences in paste viscosity. Comparison of the Argical MK and Argical* MK data reveals the influence of water content on setting time. The Argical* MK content, taking into account the reduced reactive Al in Argical MK also had reduced H_2O content to maintain a reactive H_2O:Al molar ratio of 8. The reduced water content results in higher paste viscosity, rapid initial set, and earlier final set. The geopolymer paste made using Argical MK was set rapidly, with final set after 15 hours. This was surprising because Table 2 clearly showed Argical MK contains the lowest content of reactive Si and Al and Table 4 showed it contains an intermediate Al (V) content. The longest setting time (~42 hours) was for the geopolymer made using MetaMax MK which contained the highest Al (V) content at ~ 86%.

Isothermal conduction calorimetry data (Figure 6) for the different MK geopolymer samples at 20 °C clearly shows initial heat output during the first 30 hours was highest for the Argical MK samples, followed by MetaStar MK and MetaMax MK, and these results reflect the trends observed in setting time data.

The heat output data can be separated into three exothermic regions (Granizo and Blanco, 1998 Buchwald et al., 2009, Yao et al., 2009). During early hydration the exothermic signal (A) is attributed to wetting of solid particle surfaces with the activating solution. During this process, MK is dissolved to form alumina/silica-hydroxy species and oligomers (De Silva et al., 2007, Rahier et al., 2007a). After the initial exothermic signal and a

characteristic period of minimum heat output, a second asymmetric exothermic signal (B) is observed. This indicates polymerisation in which the oligomers combine to form larger networks. A third exothermic event can be observed as a shoulder (C) (Zhang et al., 2012). This is indicative of structural stabilisation and can be seen for all geopolymer samples except those prepared from Argical MK. After 60-120 hours, dependent on the MK sample used, the geopolymerisation reaction becomes limited with only small and gradual changes occurring to the paste microstructure and chemistry.

The total heat released during the reaction over ~ 160 hours (Figure 6b) indicates that for Argical MK the total heat release reached ~120 kJ/kg after 120 hours. The total heat released for MetaStar MK and Argical* MK increased to 140 kJ/kg, whereas total heat release from MetaMax MK continued to increase to ~140 kJ/kg after 160 hours. Similar chemical reactions occur for geopolymers with a molar Al:Si:Na:H_2O ratio of 1:2:1:8. The lower total heat for Argical MK is attributed to the different effective molar Al:Si:Na:H_2O ratio. Previous research has shown that the Al:H_2O and Al:Na molar ratios influences the total heat release results (Granizo and Blanco, 1998, Granizo et al., 2000).

3.3. Effect of MK characteristics on the mechanical properties of geopolymers

It is difficult to compare the influence of different MK samples on the mechanical properties of geopolymers because these are highly dependent on the defects present, and these depend on the water content, paste viscosity and the specific mixing and casting processes used. These defects play an important role in defining geopolymer properties (Latella et al., 2008). This means that before compressive strength and flexural strength values for different geopolymer samples can be compared, the defect size has to be determined. The fracture toughness (K_{1c}) is a fundamental material property independent of

the defect size, and from the flexural strength (three-point bending test) data the critical defect size is calculated using (Clegg et al., 1990):

$$\sigma_f = \frac{K_{1c}}{0.555\sqrt{a\pi}} \quad (6)$$

where: σ_f = flexural strength (MPa) and a = defect size. The fracture toughness results obtained (Table 5) and the flexural strengths for all geopolymers are shown in Figure 7.

The K_{Ic} results are low, particularly compared to previous studies which used geopolymers with a molar Al:Si:Na:H_2O ratio of 1:2:1:7.2 (Latella et al., 2008). Flexural strength data does not vary significantly for different MK samples and the results are similar to those obtained for Portland cement pastes (Brown and Pomeroy, 1973, Hillemeier and Hilsdorf, 1977, Nallathambi et al., 1984). Flexural strengths typically range from 4 to 12 MPa, with average strengths of 7 to 8 MPa. Slightly higher values have been reported for geopolymer samples prepared using a lower water to Al ratio (Rovnaník, 2010). The results indicate that for all the geopolymer samples tested the critical defect size was between 0.5 and 2 mm.

The MK geopolymer compressive strength results (Figure 8) indicate that samples have a threshold compressive strength of ~35 MPa and a mean compressive strength of ~45 MPa. The Weibull modulus *m* calculated from these results is similar to values for concrete and granite, whereas the Weibull modulus for flexural strength is similar to that of conventional ceramics (Nallathambi et al., 1984, Prewo, 1986, Kittl et al., 1990, Tumidajski et al., 2006). Summary data from the strength testing is given in Table 6.

4. Discussion

XRD data of different MK samples indicates the presence of amorphous phases resulting from de-hydroxylation of kaolinite in commercial samples. The residual mass remaining after acid or alkali dissolution consisted of crystalline quartz, kaolin and TiO_2, and therefore the level of Si and Al in MK involved in dissolution-polymerisation reactions is related to the quantities of these impurities.

The XRF results indicate that 1% HF causes partial dissolution of quartz. This observation, coupled with the fact that MK geopolymerisation occurs in strongly alkaline environments suggests that dissolution in 8M NaOH represents a more appropriate measure of the reactive Si and Al present in MK. In both HF and NaOH dissolution experiments there was no correlation between the amount of reactive Si and Al and the Al (V) content.

The setting time and initial heat output data are correlated. The most rapid setting geopolymer paste was made with Argical MK and this MK contains significant quantities of quartz, TiO_2 and kaolinite impurities. These may act as sites for the nucleation and growth of NASH type gel from the liquid phase during geopolymerisation reactions. Many precipitation phenomena occur via nucleation and growth processes and in Portland cement pastes setting associated with CSH gel precipitation can be accelerated by seeding with inert materials or CSH gel granules (Gutteridge and Dalziel, 1990, Bronić and Subotić, 1995, Rees et al., 2008, Bullard et al., 2011). The total cumulative heat output after ~160 hours appears to provide a good indication of the degree of chemical reactivity of the MK samples during the geopolymerisation process and this correlated well with the reactive Si and Al contents determined by acid and alkali attack. A comparison of the calorimetry data for Argical MK and Argical* MK also highlights the strong influence of water content on heat output profiles. This effect can completely overshadow the more subtle differences associated with changes in the content of reactive Si and Al.

It is difficult to compare strength data between geopolymers made from different MK samples because of variations in critical defect size. However, fracture toughness measurements combined with flexural strength data have shown that all pastes contained similar critical defects. Variation in critical defect sizes occurred despite relatively long vibration of pastes during casting and use of a high Al:H_2O ratio (1:8) to ensure complete MK wetting. The smallest critical defect size was 0.25 mm and this may be reduced further by using lower water content if adequate mixing can be achieved for more viscous pastes.

The Weibull modulus for compressive strength data is relatively high which indicates testing can use a small number of replicates. The compressive strength is independent of the original Al (V) content in MK. Large variations in MK Al (V) content existed between the samples tested but compressive strengths of the geopolymers were generally very similar.

5. Conclusions

No clear correlation was found between the Al (V) content in MK samples and geopolymer setting time, heat output or strength development. Dissolution of MK in 8M NaOH can be used to determine the reactive Si and Al content. This is preferable to dissolution in 1 % HF as this causes partial dissolution of quartz impurities, leading to an overestimate of the reactive Si. The unreactive content in MK may increase the rate of initial heat output and accelerate geopolymer setting, possibly through accelerated nucleation and growth of geopolymer gel. The combination of flexural strength and fracture toughness testing can be used to calculate the critical defect size. This was found to be ~0.25 mm in MK geopolymers and this limits the resulting mechanical properties.

Acknowledgement

The authors would like to thank the Decommissioning, Immobilization and Management of Nuclear waste for Disposal (DIAMOND) consortium and the EPSRC for funding this research. We would also like to acknowledge the contribution of Dr Robert Law from the Department of Chemistry at Imperial College London.

References

Bell, J. L., Driemeyer, P. E. and Kriven, W. M., 2009a, Formation of Ceramics from Metakaolin-Based Geopolymers. Part II: K-Based Geopolymer. Journal of the American Ceramic Society 92, 607-615.

Bell, J.L., Driemeyer, P.E., Kriven, W.M., 2009b. Formation of Ceramics from Metakaolin-Based Geopolymers: Part I: Cs-Based Geopolymer. Journal of the American Ceramic Society 92, 1-8.

Bergman, B., 1984. On the estimation of the Weibull modulus. Journal of Materials Science Letters 3, 689-692.

Blackford, M.G., Hanna, J.V., Pike, K.J., Vance, E.R., Perera, D.S., 2007. Transmission Electron Microscopy and Nuclear Magnetic Resonance Studies of Geopolymers for Radioactive Waste Immobilization. Journal of the American Ceramic Society 90, 1193-1199.

Bronic, J., Subotic B., 1995. Role of homogeneous nucleation in the formation of primary zeolite particles. Microporous Materials 4, 239-242.

Brown, J.H., Pomeroy, C.D., 1973. Fracture toughness of cement paste and mortars. Cement and Concrete Research 3, 475-480.

Buchwald, A., Tatarin, R., Stephan, D., 2009. Reaction progress of alkaline-activated metakaolin-ground granulated blast furnace slag blends. Journal of Materials Science 44, 5609-5617.

Bullard, J.W., Jennings, H.M., Livingstone, R.A., Nonat A., Scherer, G.W., Schweitzer, J. S., Scrivener, K. L., Thomas, J.J., 2011. Mechanisms of cement hydration. Cement and Concrete Research 41, 1208-1223.

Cheng, T.W., Chiu, J.P., 2003. Fire-resistant geopolymer produced by granulated blast furnace slag. Minerals Engineering 16, 205-210.

Chindaprasirt, P., Chareerat, T., Sirivivatnanon, V., 2007. Workability and strength of coarse high calcium flyash geopolymer. Cement and Concrete Composites 29, 224–229.

Clegg, W.J., Kendall, K., Alford, N.M., Button, T.W., Birchall, J.D., 1990. A simple way to make tough ceramics. Nature 347, 455-457.

Davidovits, J., 2008. Geopolymer Chemistry and Applications, Saint-Quentin, France, Institut Geopolymere.

De Silva, P., Sagoe-Crenstil, K., Sirivivatnanon, V., 2007. Kinetics of geopolymerization: Role of Al_2O_3 and SiO_2. Cement and Concrete Research 37, 512-518.

Duxson, P., Provis, J.L., Lukey G.C., Mallicoat, S.W., Kriven, W.M., Van Deventer, J.S.J., 2005. Understanding the relationship between geopolymer composition, microstructure and mechanical properties. Colloids and Surfaces. A, Physicochemical and Engineering Aspects 269, 47-58.

Duxson, P., Fernandez-Jimenez, A., Provis J.L., Lukey, G.C., Palomo, A., Van Deventer, J.S.J., 2007a. Geopolymer technology: the current state of the art. Journal of Materials Science 42, 2917-2933.

Duxson, P., Lukey, G.C., Van Deventer, J.S.J., 2007b. Physical evolution of Na-geopolymer derived from metakaolin up to 1000°C. Journal of Materials Science 42, 3044-3054.

Duxson, P., Mallicoat, S.W., Lukey, G.C., Kriven, W.M., Van Deventer, J.S.J., 2007c. The effect of alkali and Si/Al ratio on the development of mechanical properties of metakaolin-based geopolymers. Colloids and Surfaces. A, Physicochemical and Engineering Aspects 292, 8-20.

Fernandez-Jimenez, A., De La Torre, A.G., Palomo, A., Lopez-Olmo, G., Alonso, M.M., Aranda, M.A.G., 2006. Quantitative determination of phases in the alkali activation of fly ash. Part I. Potential ash reactivity. Fuel 85, 625-634.

Fletcher, R.A., Mackenzie, K.J.D., Nicholson, C.L., Shimada, S., 2005. The composition range of aluminosilicate geopolymers. Journal of the European Ceramic Society 25, 1471-1477.

Granizo, M.L., Blanco, M.T., 1998. Alkaline activation of metakaolin- An isothermal conduction calorimetry study. Journal of Thermal Analysis 52, 957-965.

Granizo, M. L., Blanco-Varela, M.T., Palomo, A., 2000. Influence of the starting kaolin on alkali-activated materials based on metakaolin. Study of the reaction parameters by isothermal conduction calorimetry. Journal of Materials Science 35, 6309-6315.

403 Gutteridge, W.A., Dalziel, J.A., 1990. Filler cement: the effect of the secondary component
404 on the hydration of Portland cement: part I. A fine non-hydraulic filler. Cement and
405 Concrete Research 20, 778-782.
406 Hardjito, D., Wallah, S.E., Sumajouw, D.M.J., Rangan, B.V., 2004. On the development of
407 fly ash-based geopolymer concrete. ACI Materials Journal 101, 467-472.
408 Hermann, E., Kunze, C., Gatzweiler R., Kiebig, G., Davidovits, J., 1999. Solidification of
409 various radioactive residues by geopolymer with special emphasis on long-term-
410 stability. in Davidovits, J., Davidovits, R., James, C. (Eds.) Geopolymer '99. Saint-
411 Quentin, France, Institut Géopolymère.
412 Hillemeier, B., Hilsdorf, H.K., 1977. Fracture mechanics studies on conrete compounds.
413 Cement and Concrete Research 7, 523-536.
414 Khale, D., Chaudhary, R., 2007. Mechanism of geopolymerization and factors influencing its
415 development: a review. Journal of Materials Science 42, 729-746.
416 Khalili, A., Kromp, K., 1991. Statistical properties of Weibull estimators, Journal of
417 Materials Science 26, 6741-6752.
418 Kittl, P., Leon, M., Diaz, G., Lillo, A., 1990. Probabilistic compressive strength of sound dry
419 granite. Rock Mechanics and Rock Engineering 23, 21-28.
420 Komnitsas, K., Zaharaki, D., 2007. Geopolymerisation: A review and prospects for the
421 minerals industry. Minerals Engineering 20, 1261-1277.
422 Kuenzel, C., Vandeperre, L., Cheeseman, C.R., Boccaccini, A.R., 2010. Geopolymers for the
423 encapsulation of solid nuclear waste. Decommissioning, Immobilisation and
424 Management of Nuclear Waste Disposal 2010 Manchester, UK.
425 Kuenzel, C., Cheeseman, C.R., Vandeperre, L., Donatello, S., Boccaccini, A.R., 2012. An
426 assessment of drying shrinkage in metakaolin-based geopolymers. Journal of the
427 American Ceramic Society 95, 3270-3277.
428 Kuenzel, C., 2013. Nuclear waste encapsulation using metakaolin based geopolymers.
429 Department of Civil and Environmental Engineering. PhD thesis. Imperial College
430 London.
431 Latella, B.A., Perera, D.S., Durce, D., Mehrtens, E.G., Davis, J., 2008. Mechanical properties
432 of metakaolin-based geopolymers with molar ratios of Si/Al 2 and Na/Al 1. Journal of
433 Materials Science 43, 2693-2699.
434 Lawn, B. R., Wilshaw, T.R., 1975. Fracture of brittle solids, Cambridge, Cambridge
435 University Press.

436 Massiot, D., Fayon, F., Capron, M., King, I., Le Calve, S., Alonso, B., Durand, J.O., Bujoli,
437 B., Gan, Z., Hoatson, G., 2002. Modelling one and two-dimensional solid-state NMR
438 spectra. Magnetic resonance in chemistry 40, 70-76.
439 Masson, J.J., Bourgain, E., 1992. Some guidelines for a consistent use of the Weibull
440 statistics with ceramic fibres. International Journal of Fractures 55, 303-319.
441 Nallathambi, P., Karihaloo, B.L., Heaton, B.S., 1984. Effect of specimen and crack sizes,
442 water/cement ratio and coarse aggregate texture upon fracture toughness of concrete
443 Magazine of Concrete Research 36, 227-236.
444 Palomo, A., Grutzeck, M.W., Blanco, M.T., 1999a. Alkali-activated fly ashes - A cement for
445 the future. Cement and Concrete Research 29, 1323-1329.
446 Palomo, A., Blanco-Varela, M.T., Granizo, M.L., Puertas, F., Vazquez, T., Grutzeck, M.W.,
447 1999b. Chemical stability of cementitious materials based on metakaolin. Cement and
448 Concrete Research 29, 997-1004.
449 Perera, D.S., Aly, Z., Vance, E.R., Mizumo, M., 2005. Immobilization of Pb in a geopolymer
450 matrix. Journal of the American Ceramic Society 88, 2586-2588.
451 Perera, D.S., Vance, E.R., Aly, Z., Davis, J., 2006. Immobilization of Cs and Sr in
452 geopolymers with Si/Al molar ratio of ~2. Ceramic Transitions 176, 91-96.
453 Poulesquen, A., Frizon, F., Lambertin, D., 2011. Rheological behavior of alkali-activated
454 metakaolin during geopolymerization. Journal of Non-Crystalline Solids 357, 3565-
455 3571.
456 Prewo, K.M., 1986. Tension and flexural strength of silicon carbide fibre-reinforced glass
457 ceramics. Journal of Materials Science 21, 3590-3600.
458 Provis, J.L., Lukey, G.C., Van Deventer, J.S.J., 2005. Do geopolymers actually contain
459 nanocrystalline zeolites? A reexamination of existing results. Chemistry of Materials
460 17, 3075-3085.
461 Rahier, H., Wastiels, J., Biesemans, M., Willem, R., Van Assche, G., Van Mele, B., 2007a.
462 Reaction mechanism, kinetics and high temperature transformations of geopolymers.
463 Journal of Materials Science 42, 2982-2996.
464 Rahier, H., Denayer, J.F., Van Mele, B., 2007b. Low-temperature synthesized aluminosilicate
465 glasses Part IV Modulated DSC study on the effect of particle size of metakaolinite on
466 the production of inorganic polymer glasses. Journal of Materials Science 38, 3131-
467 3136.

Rees, C.A., Provis, J.L., Lukey, G.C., Van Deventer, J.S.J., 2008. The mechanism of geopolymer gel formation investigated through seeded nucleation. Colloids and Surfaces A: Physicochemical and Engineering Aspects 318, 97-105.

Rooke, D.P., Cartwright, D.J., 1976. Compendium of stress intensity factors, London, UK, Her Majesty's Stationary Office.

Rovnanik, P., 2010. Effect of curing temperature on the development of hard structure of metakaolin-based geopolymer. Construction and Building Materials 24, 1176-1183.

Rowles, M., O'Conner, B., 2003. Chemical optimisation of the compressive strength of aluminosilicate geopolymers synthesised by sodium silicate activation of metakaolinite. Journal of Materials Chemistry 13, 1161-1165.

Ruiz-Santaquiteria, C., Fernandez-Jimenez, A., Palomo, A., 2011. Quantitative determination of reactive SiO_2 and Al_2O_3 in aluminosilicate materials. 13th International Congress on the Chemistry of Cement, Madrid, Spain.

Sagoe-Crentsil, K., Weng, L., 2007. Dissolution processes, hydrolysis and condensation reactions during geopolymer synthesis: Part II. High Si/Al ratio systems. Journal of Materials Science 42, 3007-3014.

Sanz, J., Madani, A., Serratosa, J.M., Moya, J.S., Aza, S., 1988. Aluminum-27 and silicon-29 magic-angle spinning nuclear magnetic resonance study of the kaolinite-mullite transformation. Journal of the American Ceramic Society 71, C-418-C-421.

Somna, K., Jaturapitakkul, C., Kajitvichyanukul, P., Chindaprasirt, P., 2011. NaOH-activated ground fly ash geopolymer cured at ambient temperature. Fuel 90, 2118-2124.

Standard, 2008. Methods of testing cement -Part 3: Determination of setting times and soundness. B.S. (Ed.) BS EN 196-3:1995. British Standards Institution.

Tumidajski, P.J., Fiore, L., Khodabocus, T., Lachemi, M., Pari, R., 2006. Comparison of Weibull and normal distributions for concrete compressive strengths. Canadian Journal of Civil Engineering 33, 1287-1292.

Van Jaarsveld, J.G.S., Van Deventer, J.S.J., Lukey, G.C., 2004. A comparative study of kaolinite versus metakaolinite in flyash based geopolymers containing immobilized metals Chemical Engineering Communications 191, 531-549.

Weibull, W., 1951. A statistical distribution function of wide applicability. Journal of Applied Mechanics 18, 293-297.

Yao, X., Zhang, Z., Zhu, H., Chen, Y., 2009. Geopolymerization process of alkali–metakaolinite characterized by isothermal calorimetry. Thermochimica Acta 493, 49-54.

Zhang, Z., Wang, H., Provis, J.L., Bullen, F., Reid, A., Zhu, Y., 2012. Quantitative kinetic and structural analysis of geopolymers. Part 1. The activation of metakaolin with sodium hydroxide. Thermochimica Acta 539, 23-33.

Table 1
Mass content of SiO_2 and Al_2O_3 in the three metakaolin samples used in this work, determined by XRF with the expressed as mass percent (%) as oxides.

	SiO_2	Al_2O_3	other oxides	LOI	mean particle size [µm]
MK MetaStar 501	56.0	38.1	5.1	0.8	5.4
MK Argical M1200	55.0	39.0	4.9	1.0	6.5
MK MetaMax	53.0	43.8	3.1	1.0	4.4

Table 2
The weight of the residues remaining after 20 hours dissolution in either 8 M NaOH or 1 wt.% HF (in wt.%) for the three metakaolin samples. Results are the average of three measurements.

	mass %		
	MetaStar MK	Argical MK	MetaMax MK
HF (1%)	1.8	18.7	2.2
NaOH (8M)	3.6	21.7	4.4

Table 3
XRF analysis of Argical MK before and after HF or NaOH attack (results in wt%). Based on Table 2 and the XRF results after dissolution, the reactive Al and Si amounts in Argical MK were calculated and results are noted as Argical* MK.

	SiO_2	Al_2O_3	Na_2O + K_2O	CaO + MgO	TiO_2	Fe_2O_3	LOI
Argical MK	55	39	1	0.6	1.5	1.8	1
residue Argical (in NaOH)	60.3	20.2	4.5	0.2	7.9	1.6	2.9
residue Argical (in HF)	55.7	19.5	3.6	0.4	8.5	1.3	4.3
Argical* MK (reactive, based on NaOH results)	43	35					

Table 4
Percentage of different Al coordination determined using ^{27}Al-NMR in the different metakaolin samples.

%	Al(IV)	Al(V)	Al(VI)
MK MetaStar 501	20.1	43.7	36.2
MK Argical	17.4	70.4	1.9
MK MetaMax	10.8	86.0	3.2

Table 5
Fracture toughness of MK based geopolymers after 56 days curing. Results were calculated using Equation 1 and 2. Average results determined from 6 measurements.

Geopolymer	K_{Ic} [MPa/m^2]	
	average	STDEV
MetaStar MK	0.22	0.03
MetaMax MK	0.20	0.01
Argical MK	0.24	0.02
Argical* MK	0.24	0.02

Table 6
Weibull modulus for compressive and flexural strength, as well as average and median strength of metakaolin based geopolymers.

metakaolin	MetaMax MK	MetaStar MK	Argical* MK	Argical MK
	Compressive strength [MPa]			
Weibull modulus (*m*)	13.1	10.5	12.3	12.2
characteristic strength (σ_0)	53.4	50.7	48.4	44.1
Average strength	51.4	47.5	46.5	42.3
STDEV	4.7	5.4	4.6	4.2
median	50.7	48.3	46	41.7
	Flexural strength [MPa]			
Weibull modulus (*m*)	3.7	4.2	5.4	5.6
characteristic strength (σ_0)	8.8	7.9	8.8	8.3
Average strength	8.0	7.3	8.1	7.6
STDEV	2.1	1.6	1.7	1.8
median	8.0	7.1	8.2	7.4

Figure

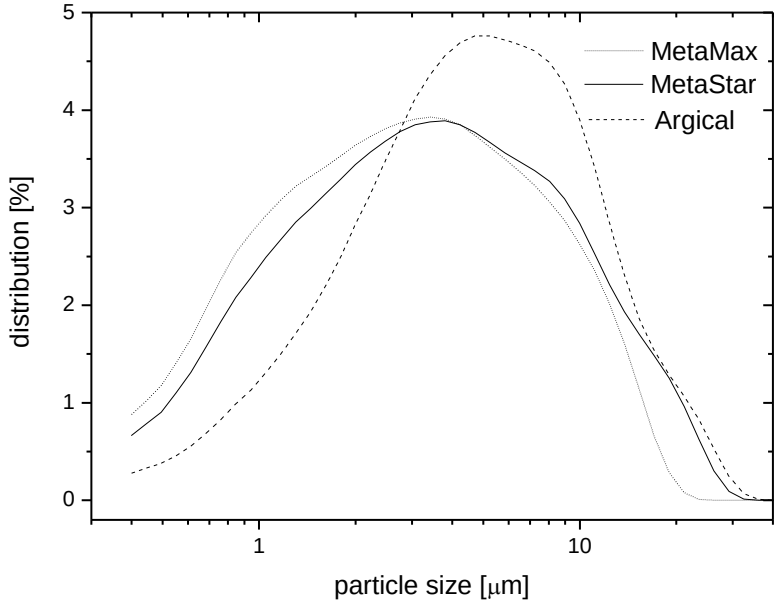

Fig. 1. Particle size distribution of metakaolin (MK) samples used in this study.

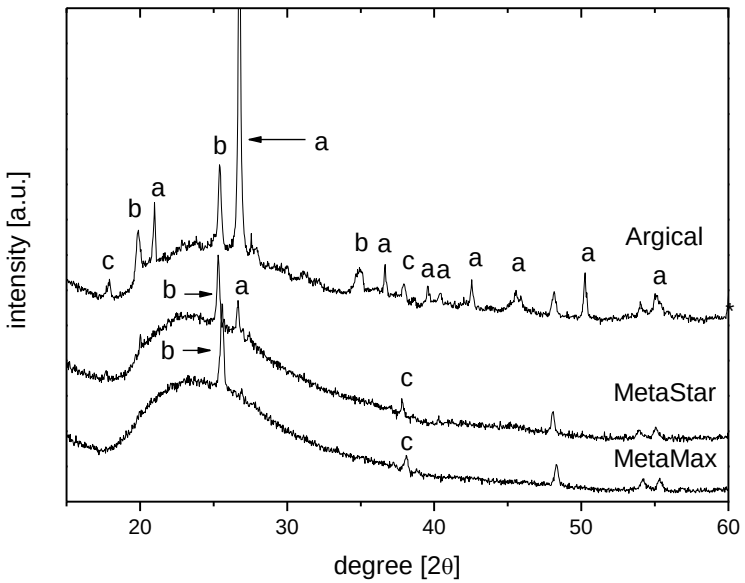

Fig. 2. X-ray diffraction (XRD) of the three metakaolin samples; a = quartz low (Ref. Code 00-005-0490), b = SiO_2, (Ref. Code 01-080-2147), c = kaolinite (Ref. Code 00-006-0221).

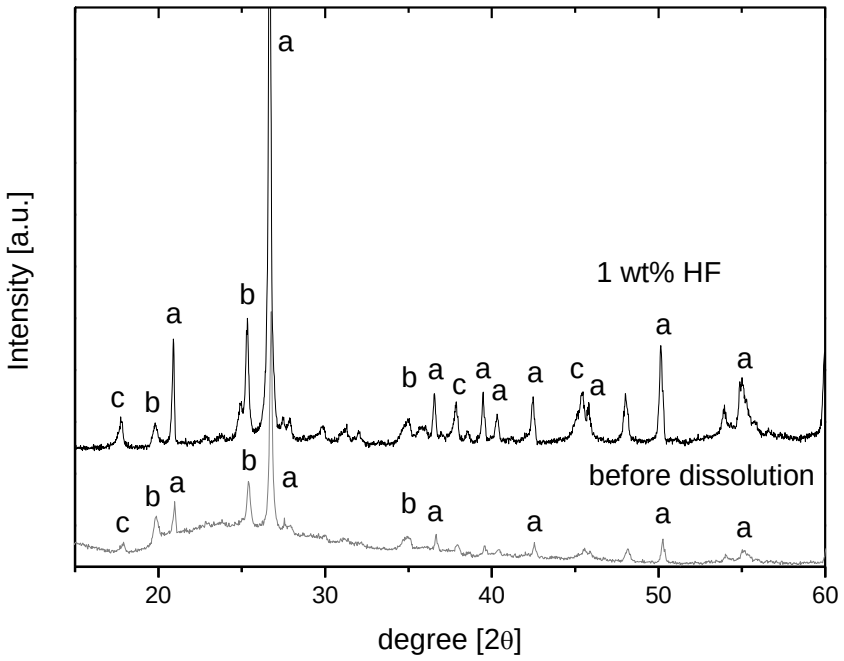

Fig. 3. X-ray diffraction data for as-received Argical MK and the residue after dissolution in HF.
a = quartz low (Ref. Code 00-005-0490), b = SiO_2, (Ref. Code 01-080-2147), c = kaolinite (Ref. Code 00-006-0221)

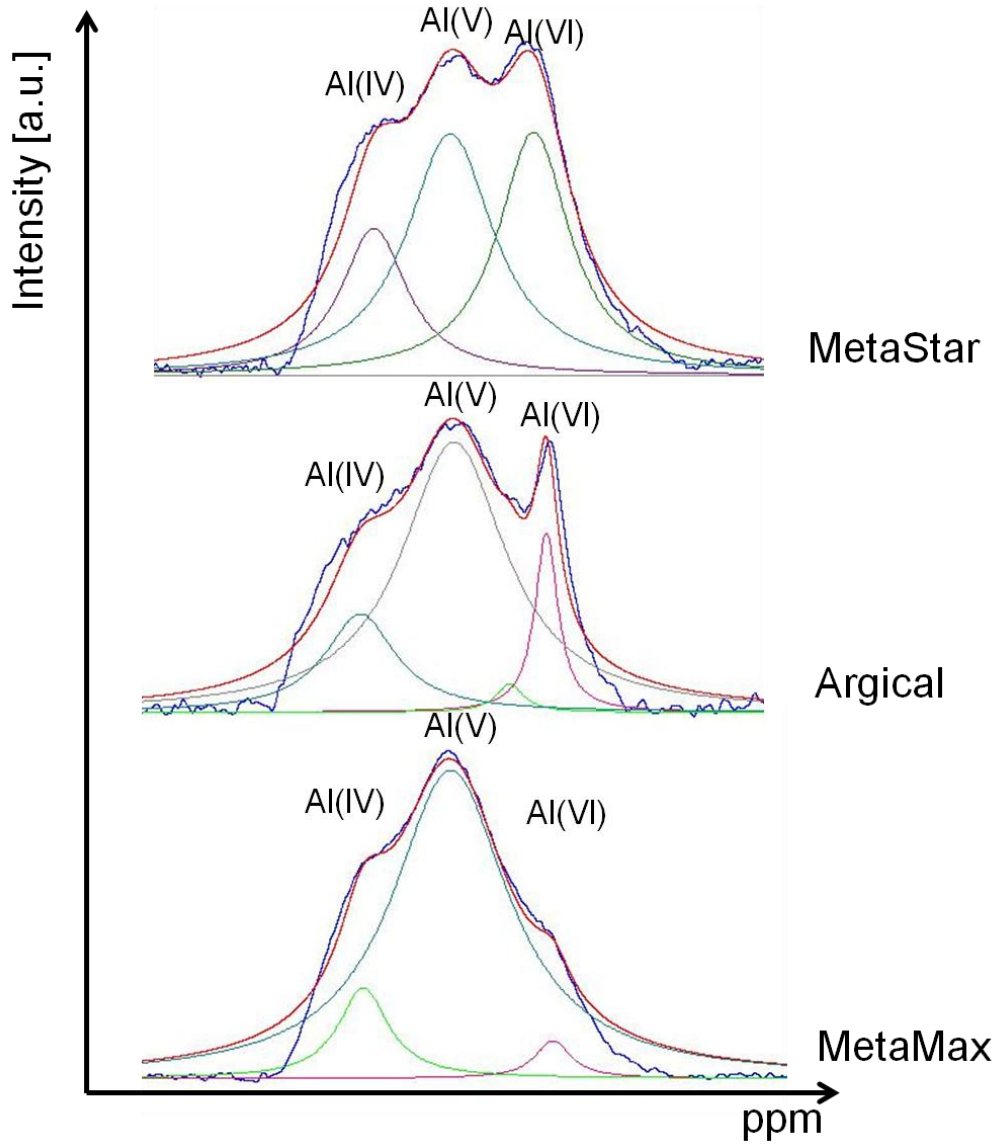

Fig. 4. ^{27}Al-NMR results including the Gaussian fit to determine the amount of different Al coordination numbers in metakaolin.

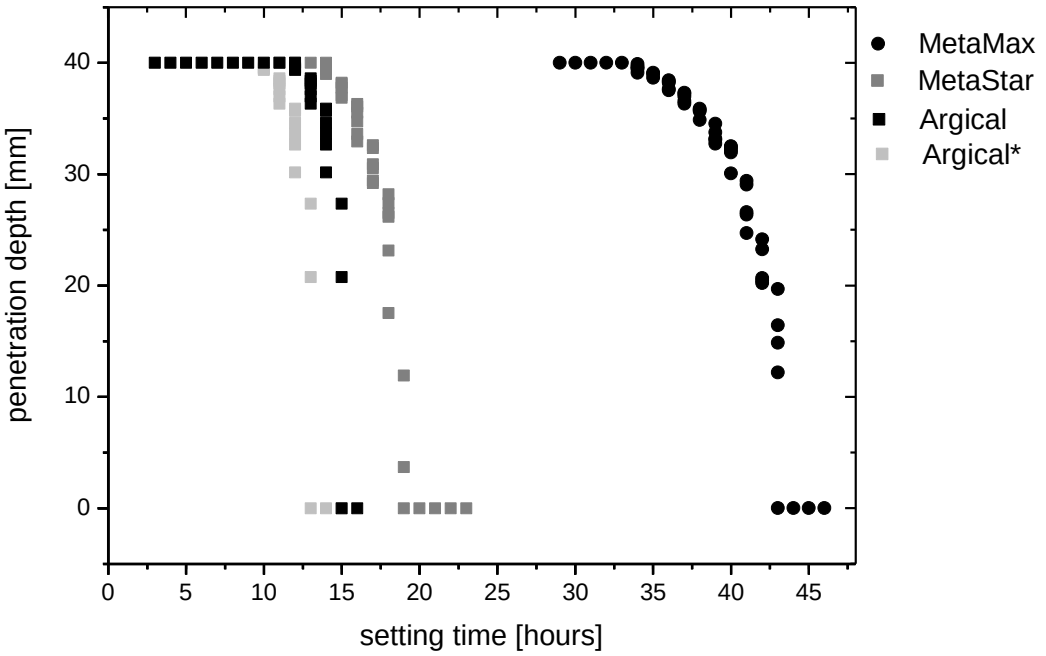

Fig. 5. The setting characteristics of metakaolin geopolymers made with different metakaolin samples determined using a Vicat needle penetrometer.

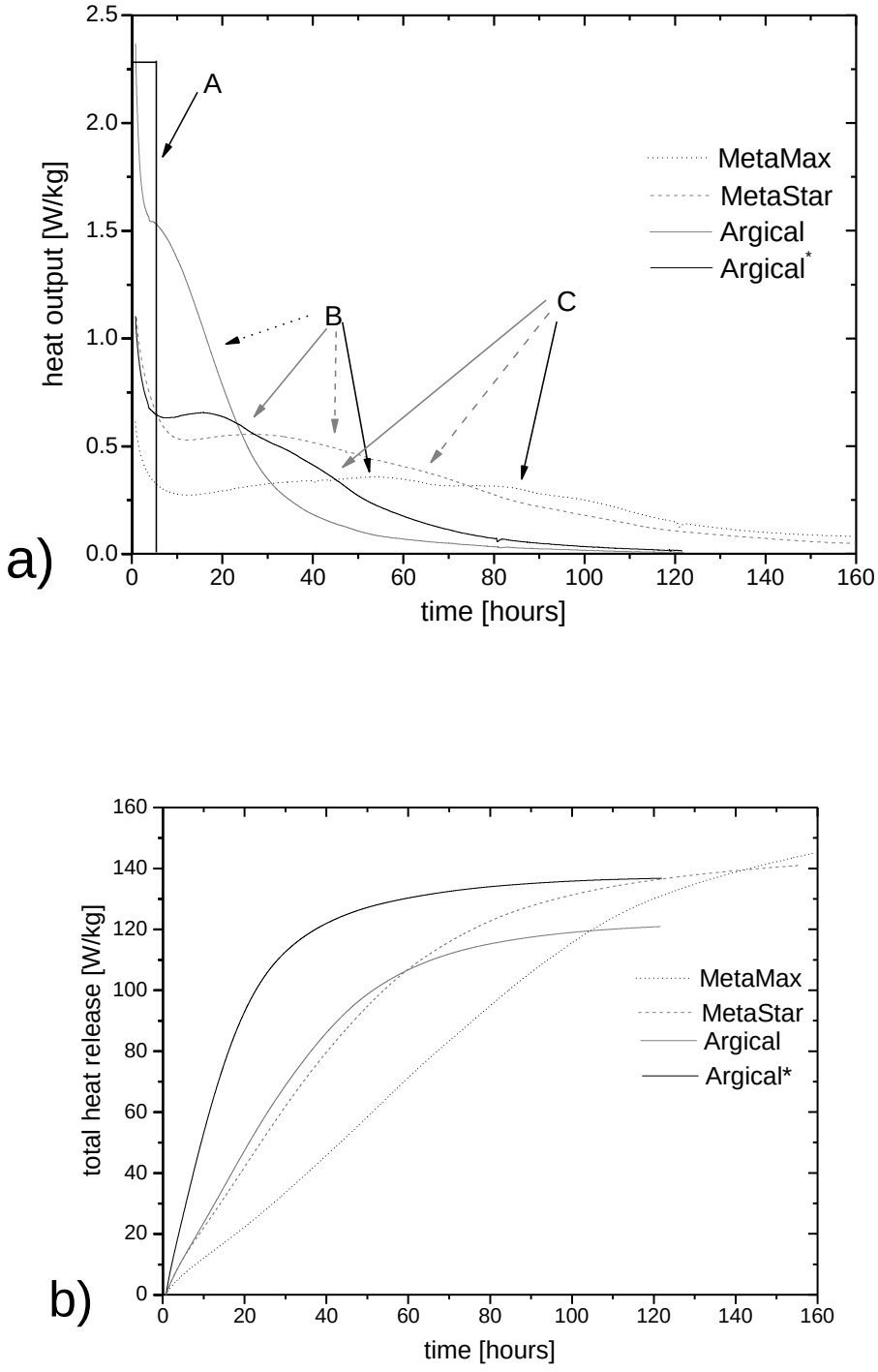

Fig. 6. Isothermal conduction calorimetry data for metakaolin based, a) rate of heat output versus time where A = wetting of metakaolin particles, B = polymerization of oligomers to form a larger network and C = structural stabilization of larger network; b) cumulative heat output versus time.

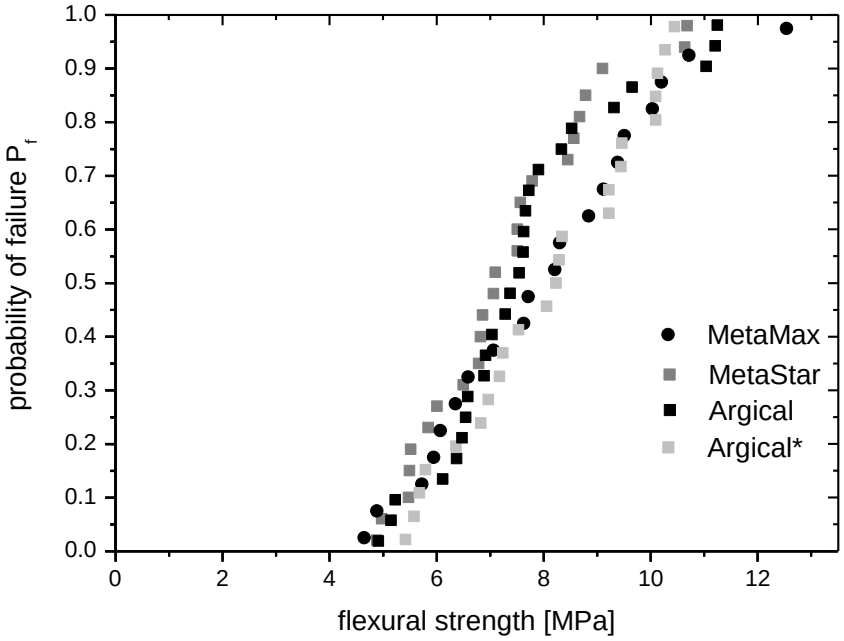

Fig. 7. Weibull plots of flexural strength values for all metakaolin geopolymer paste samples plotted against the probability of failure, calculated using Equation 4.

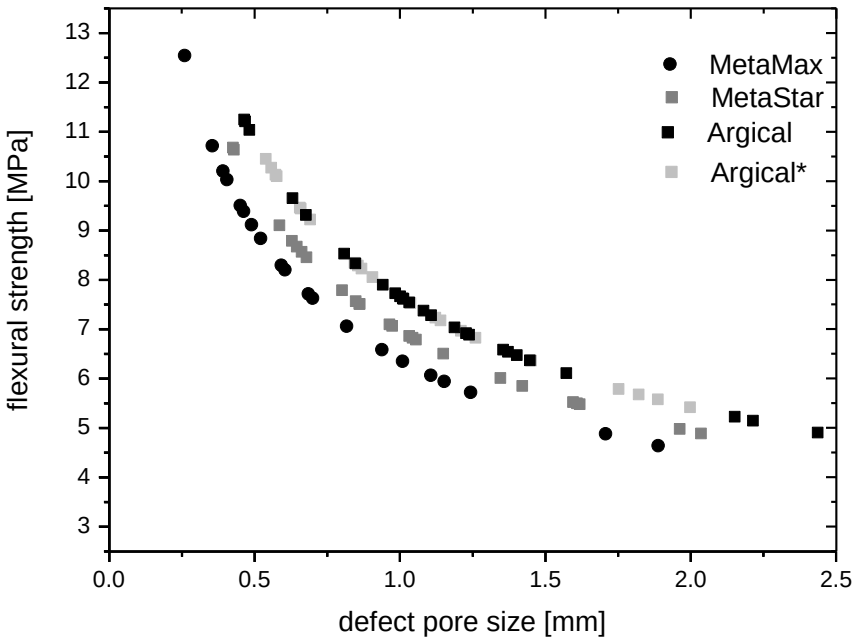

Fig. 8. The variation of flexural strength with critical defect pore size in metakaolin geopolymer pastes calculated by using Equation 6.

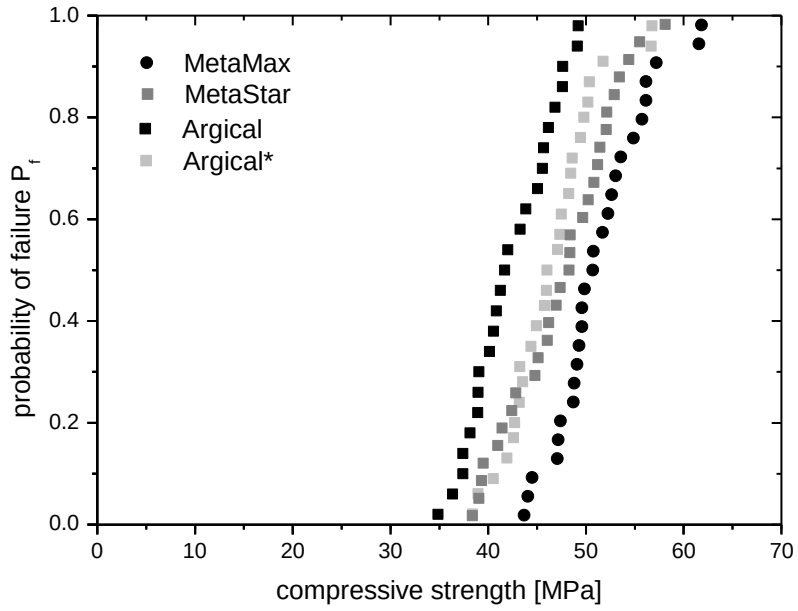

Fig. 9. Weibull statistics data showing the compressive strength for all metakaolin geopolymers after curing for 56 days.

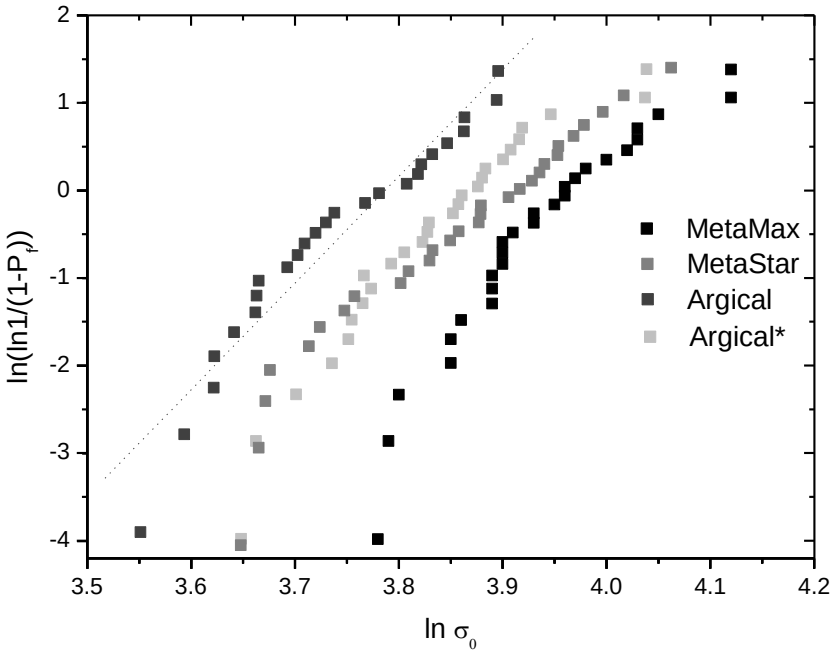

Fig. 10. Weibull data used to calculate the Weibull modulus *m* (slope of the lines), showing the compressive strength data for metakaolin geopolymers.